21 March 1996

PHYSICS LETTERS B

ELSEVIER

Physics Letters B 371 (1996) 25-33

# Parity violation in the $\gamma$-decay of polarized $^{93}$Tc nuclei in the 17/2$^-$ isomeric state

M. Hass [a], C. Broude [a], L. Weissman [a], L. Müller [b], G. Montagnoli [b], F. Scarlassara [b], G.F. Segato [b], C. Signorini [b], G. Goldring [c,1], D. Ackermann [c], P. Bednarczyk [c], L. Corradi [c], P. Spolaore [c], M. Lindroos [d], S. Hofmann [e], V. Ninov [e], F.P. Hessberger [e], F. Soramel [f], N. Takahashi [g], B.A. Brown [h]

[a] Department of Particle Physics, Weizmann Institute of Science, Rehovot, Israel
[b] Universita di Padova and INFN, Sezione di Padova, Italy
[c] INFN, Laboratori Nazionali di Legnaro, Italy
[d] CERN, Geneva, Switzerland
[e] GSI, Darmstadt, Germany
[f] Universta di Udine and INFN, Sezione di Triesta, Italy
[g] Osaka University, Osaka, Japan
[h] National Superconducting Cyclotron Laboratory and Department of Physics and Astronomy, Michigan State University, East Lansing, MI 48824, USA

Received 25 September 1995; revised manuscript received 11 December 1995
Editor: J.P. Schiffer

**Abstract**

We report on a determination of the parity nonconserving (PNC) matrix element in the bound parity doublet $\frac{17}{2}^- - \frac{17}{2}^+$ of $^{93}$Tc. The experiment was carried out at the GSI, Darmstadt and LNL, Legnaro laboratories. The recoil-mass-separated radioactive beam of $^{93}$Tc nuclei in the $\frac{17}{2}^-$ isomer, following a fusion-evaporation reaction, was polarized by the tilted-foil method and the resulting 0°-180° $\gamma$ asymmetry with respect to the induced polarization direction was measured by two large-volume Ge detectors. The measured $\gamma$ asymmetry of 3-$\sigma$ significance, $A_\gamma = 8.4(2.7)\cdot 10^{-4}$, yields a matrix element of $|\langle\frac{17^-}{2}|H_{\rm pnc}|\frac{17^+}{2}\rangle| = 0.59(19)(25)$ meV. This experimental result is compared to microscopic calculations based on the DDH "best value" interaction for the nuclear weak Hamiltonian. We discuss our results and their significance with respect to the existing data regarding PNC effects in bound nuclear systems.

*PACS:* 21.10.Ky; 21.10.Pc; 23.40.Hc

The $\frac{17}{2}^-$ isomeric level of $^{93}$Tc has a $\frac{17}{2}^+$ partner at a separation of only 300 eV [1,2]. The isomer decays to a $\frac{13}{2}^+$ state through a mixed M2/E3 transition. Any contribution of the opposite parity $\frac{17}{2}^+$ state would lead to an E2 admixture to the transition whose intrinsic transition matrix element is larger by a factor of ~1000 than M2 and E3. For a polarized sample of the isomer, the mixed parity component in the transition introduces a $P_1(\cos\theta)$ term in the angular distribution

[1] Permanent address: Department of Particle Physics, Weizmann Institute of Science, Rehovot, Israel.


*SSDI* 0370-2693(95)01596-5

with respect to the direction of polarization, yielding a 0°–180° asymmetry $A_\gamma$ of the decay $\gamma$-rays. The detection of this small asymmetry and its implication for establishing and understanding PNC in a bound nuclear system is the subject of this publication.

Parity nonconservation originates at the most fundamental level from the weak currents mediated by the exchange of the $W$ and $Z$ bosons. PNC in nuclei was the first place where the nonstrangeness-changing sector of the standard weak-interaction model was observed [3]. Nuclear PNC is usually interpreted in terms of the underlying nucleon-nucleon (NN) PNC interaction. Theoretical "best value" strengths of NN PNC interactions were established by Desplanques, Donoghue and and Holstein (DDH) [4] and their hadronic model dependence has been investigated [4,5].

In order to experimentally establish the strengths of the isoscalar (IS), isovector (IV) and isotensor (IT) components of the NN PNC interaction, it is important to compare results from NN scattering with those from nuclear bound states. The interpretation of the results for the nuclear bound states depends upon accurate nuclear-structure calculations. For a few nuclei, such as $^{18}$F and $^{19}$F, much of the nuclear-structure uncertainty can be removed by comparison to the analogue axial-charge beta decays [3], and in general for light nuclei large-scale shell-model calculations can be carried out [3,6]. The upper limit for the empirical strength of the IV component found from light nuclei [6] is a factor of three smaller than the DDH "best value" based upon the SU(3) quark model plus penguin-diagram corrections. This is surprising because it is this component which was predicted to be enhanced by the neutral current, $Z$-boson, contribution which is unique to the nonstrangeness changing PNC [4]; never-the-less, it is still within the range allowed by hadronic models [4].

There are a number of cases, such as in $^{180}$Hf [7], where nuclear PNC has been observed, but where the interpretation is limited by the uncertainties in the nuclear wave functions [3]. Recently, large PNC effects in low-energy neutron scattering have been observed, and the interpretation of the results for these compound nucleus states has focused on the nuclear many-body "enhancement" factor [8]. All bound-state cases studied to date are thought to be dominated by the "one-body" nuclear mechanism which originates from a coherent average of the NN PNC interaction over all core nucleons and which yields single-particle matrix elements $\langle l,j|V_{PNC}|l-1,j\rangle$ on the order of one eV

The case of $^{93}$Tc presents a unique situation. The structure of the nuclei with 50 neutrons ($N=50$) including $^{93}$Tc are well described by shell-model wave functions [9,10], and thus reasonable nuclear-structure calculations can be carried out, although not at the same level of completness as those for light nuclei. It is different from the cases studied in light nuclei because it is a high-spin doublet and because there is (in the simplest model) no "one-body" component – it is entirely two-body. In particular, we will show below that the $^{93}$Tc PNC is particularly sensitive to the isotensor component of the NN PNC potential.

A full description of the essentials of the experiments, including the method of tilted-foil polarization of separated isomer beams can be found in Ref. [11]. We briefly summarize the salient points. The energy level spectrum of $^{93}$Tc is shown in Fig. 1. The close proximity of the $\frac{17}{2}^-$ and $\frac{17}{2}^+$ levels favors a mixing of the wave functions if the parity violating matrix element $\langle \frac{17}{2}^- | H_{\rm pnc} | \frac{17}{2}^+ \rangle$ is finite. For the $\frac{17}{2}^-$ state, the parity mixed wave function leads to an E2 admixture in the predominant M2/E3 gamma transition to the $\frac{13}{2}^+$ level. The sensitivity to the parity mixing is strongly enhanced due to the intrinsically more intense E2 strength. The parity admixture yields an $A_1 P_1(\cos\theta)$ term in the angular distribution of the gamma-rays with respect to the direction of polarization [2]. The measured anisotropy coefficient is given by: $A_\gamma = A_1 Q_1 \sqrt{3} p_I$ where $Q_1$ is the geometrical attenuation coefficient due to the finite size of the Ge's and $p_I = \frac{\langle I_z \rangle}{\sqrt{I(I+1)}}$. Following the derivation in Ref. [11] and references therein, the $H_{\rm pnc}$ matrix element is given by:

$$A_1 = \frac{2\epsilon}{1+\delta^2}\,(-0.61 - 0.54\delta)$$

where $\delta$ is the E3/M2 mixing ratio of the $\frac{17}{2}^- \rightarrow \frac{13}{2}^+$ transition and $\epsilon$ is given by:

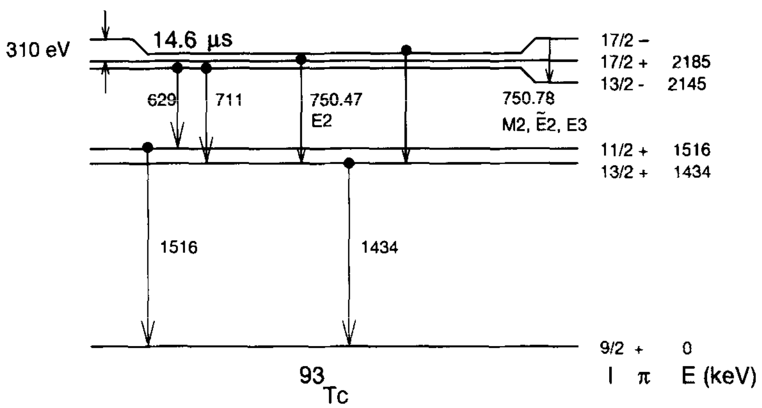


Fig. 1. The energy-level spectrum of $^{93}$Tc. The $\frac{17}{2}^-$ isomer and its $\frac{17}{2}^+$ parity-partner are shown. The gamma rays depopulating the $\frac{17}{2}^-$ isomer (629 keV, 711 keV, 751 keV, 1434 keV and 1516 keV) are indicated. The only transition which is expected to exhibit a PNC asymmetry (see text) is the 751 keV.

$$\epsilon = \frac{\langle \frac{13}{2}^+ | \tilde{E}2 | \frac{17}{2}^- \rangle}{\langle \frac{13}{2}^+ | M2 | \frac{17}{2}^- \rangle} = \frac{\langle \frac{17}{2}^- | H_{\text{pnc}} | \frac{17}{2}^+ \rangle}{\left[ E_{\frac{17}{2}^-} - E_{\frac{17}{2}^+} \right]} \, \frac{\langle \frac{13}{2}^+ | E2 | \frac{17}{2}^+ \rangle}{\langle \frac{13}{2}^+ | M2 | \frac{17}{2}^- \rangle}$$

with the enhancement factor:

$$\frac{\langle \frac{13}{2}^+ | E2 | \frac{17}{2}^+ \rangle}{\langle \frac{13}{2}^+ | M2 | \frac{17}{2}^- \rangle} = 2.0(7) \cdot 10^3$$

we obtain:

$$|\langle \tfrac{17}{2}^- | H_{\text{pnc}} | \tfrac{17}{2}^+ \rangle| = 91(28) \frac{|A_\gamma|}{p_I Q_1} \text{ meV} \qquad (1)$$

Experiments were carried out at the SHIP velocity filter of Gesellschaft für Scherionenforschung (GSI) (1 run) and the recoil mass spectrometer (RMS) of the Laboratori Nazionali di Legnaro (LNL) (2 runs). The results of the GSI run have been published previously in Ref. [11]. The $^{93}$Tc isomers were produced using the reactions $^{34}$Sc ($^{52}$Cr, 2p2n)$^{93}$Tc (GSI) and $^{65}$Cu($^{32}$S, 2p2n) $^{93}$Tc (LNL). A schematic view of both the GSI and the LNL experiments is shown in Figs. 2. In both cases, a heavy-ion reaction populates the $\frac{17}{2}^-$ isomer. A target wheel (GSI) or eccentric rotation device (LNL) allows an intense particle beam to be focused on the target without thermal damage. A velocity-filter/recoil mass-separator separates and transfers $^{93}$Tc isomers to the focal-plane area where they are polarized by a tilted multi-foil array and consequently stopped in a perturbation-free Pb stopper. The parameters of the RMS (SHIP) were adjusted for maximum transmission of $^{93}$Tc nuclei to the Pb stopper by monitoring the separated particles in a position-sensitive detector placed at the entrance to the foil stack and by counting isomer $\gamma$ lines. A Si particle detector was placed at the position of the Pb stopper to check the energy of $^{93}$Tc nuclei after their passage through the foils. Decay $\gamma$-rays were detected at 0° and 180° to the induced-polarization direction by two large-volume Ge detectors placed to the left and the right of the isomer beam. As already mentioned in Ref. [11], this arrangement allows for very clean $\gamma$ spectra, a very intense beam on target (high production rate) and negligible heat deposition in the foils. In all three runs we have used 16 foils of about $3\mu g/cm^2$ of collodion with a $\sim 3\mu g/cm^2$ layer of C evaporated on the exit surface. The foils were tilted by 70° with respect to the isomer-beam direction. There are a number of differences in the experimental conditions at GSI and LNL but the important features – the isomer entrance velocity to the foil stack (via the use of an energy degrader at GSI) and the structure of the stack – are very similar and so one expects the isomer polarization and the front-to-back asymmetry in the gamma angular distribution to be similar.

In order to provide a measurement that is independent of the relative efficiency of the two detectors and beam-curent fluctuations, the direction of polarization

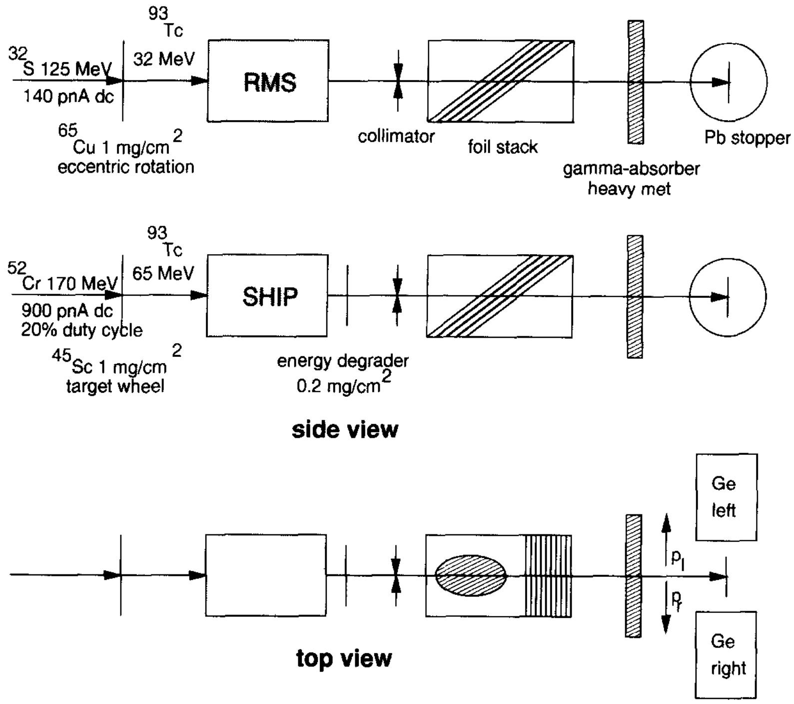


Fig. 2. A schematic representation of the experiments at GSI and LNL. The various components of the experimental arrangement are shown. The side view presents the differences between the GSI and LNL experimental parameters while the top view presented is common to both. 16 foils, tilted by 70° to the isomer-beam direction, were used at both GSI and LNL.

was switched every 5 minutes by rotating the foil stack by 180° and the double ratio DR was recorded:

$$\mathrm{DR} = \sqrt{\frac{(\mathrm{rl})}{(\mathrm{rr})} \Big/ \frac{(\mathrm{ll})}{(\mathrm{lr})}} = \frac{W(\pi)}{W(0)} \qquad (2)$$

where (rr), (lr) refer to counts in the right (left) detector for right-polarized isomers etc.

The coefficient $A_\gamma$ is then measured by the ratio:

$$\frac{W(\pi)}{W(0)} = \frac{1 - A_\gamma}{1 + A_\gamma}$$

The interaction of the foil stack with the isomer beam (scattering, absorption) can give rise to artifacts in the DR. Due to the complete left-right symmetry in the design of the apparatus one would expect asymmetries to arise only perpendicular to the beam-gamma detector plane with no component along the right-left axis as in Eq. (2); however, small angular misalignments cannot be avoided and contribute a small component of the inherently up-down asymmetry to the right-left DR [11].

There are two possible sources of $\gamma$ radiations that can lead to artifact DR's: a) the stopper: scattering in the tilted foils will lead to an asymmetric beam spot which rotates with the foils, and b) the foil stack (if the absorber in Fig. 2 is not thick enough to effectively shield the detectors from the stack); isomers stopped in the foils or – after scattering – in the frames will in general be asymmetrically located. The artifact DR can be monitored by other isomer lines in the $\gamma$ spectrum.

To derive the true DR we form a triple ratio:

$$\mathrm{TR}(i) = \frac{\mathrm{DR}(i)}{\overline{\mathrm{DR}}(i \neq 751)}$$

where i goes over all isomer lines in the spectrum and $\overline{\mathrm{DR}}(i \neq 751)$ is the average DR of all isomer lines excluding 751 keV. As all other isomer lines (except the 751 keV) do not exhibit a PNC asymmetry, the TR(751) eliminates the (small) effects mentioned above. The $A_\gamma$ parameter defined above is thus:

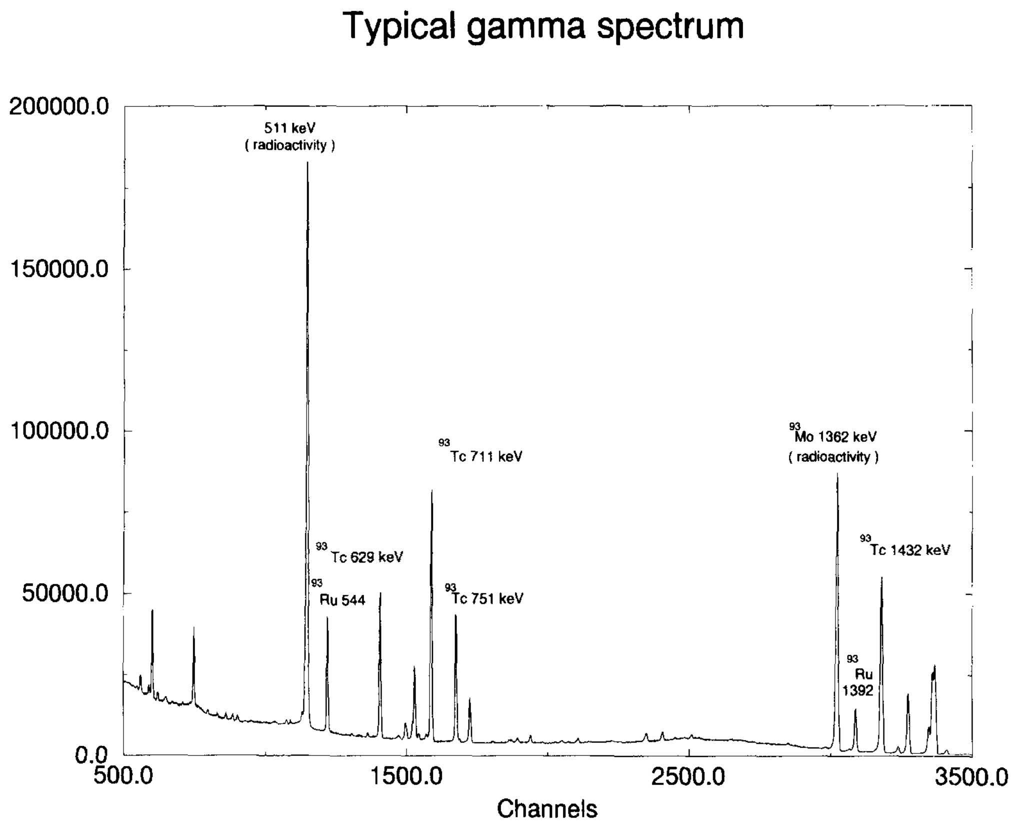


Fig. 3. A gamma spectrum for one of the Ge detectors used in the second LNL run. The gamma lines present are from the isomer decay of the $\frac{17}{2}^-$ and $\frac{21}{2}^+$ isomers of $M = 93$ nuclei ($^{93}$Tc and $^{93}$Ru, respectively), as well as lines from the ground-state radioactive decay of these nuclei.

$$A_\gamma = \frac{1 - \overline{\mathrm{TR}}(751)}{1 + \overline{\mathrm{TR}}(751)}$$

We present here results of three runs, one at GSI and two at LNL in 1994 and 1995. Fig. 3 presents the gamma spectrum of the last LNL run.

The 1362 keV line (see Fig. 3) of the 2.1 h decay of $^{93}$Tc was used to monitor, after the run, the deposition of $^{93}$Tc on the Pb stopper, the foil stack and the entrance collimator, and it was established that of the $\gamma$'s reaching the Ge detectors only a very small fraction originated in locations other than the Pb stopper.

The double and triple ratios of the isomer lines in the spectrum (average of all three runs) are shown in Fig. 4 and in Table 1. We would like to emphasize that the raw double ratios of the GSI and the LNL runs are all close to unity; hence, the renormalization associated with forming TR($i$) is small – demonstrating the quality and validity of the procedure discussed above. The resulting TR's are consistent and the average value for the totality of the data is: $1 - \overline{\mathrm{TR}}(751) = 1.68(55) \cdot 10^{-3}$ and $A_\gamma = 8.4(2.7) \cdot 10^{-4}$.

An estimate for the polarization under identical experimental conditions has been obtained in a quadrupole interaction measurement for the $8^+$ isomer of $^{92}$Mo in Rochester [12]. This has yielded the value:

$$p_I = 0.15(3)$$

The geometric attenuation coefficient in all three runs was ~0.85. With these values we derive the PNC matrix element from (1) as:

$$|\langle \frac{17^-}{2} | H_{\mathrm{pnc}} | \frac{17^+}{2} \rangle| = 0.59(19)(25)\ \mathrm{meV}$$

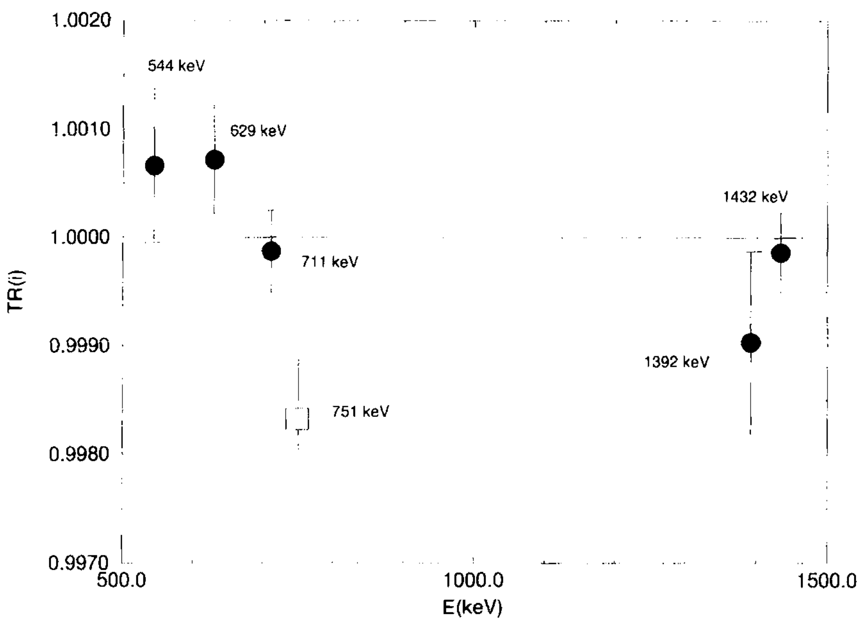


Fig. 4. The triple ratios (TR($i$)) as defined in the text of isomer lines ($^{93}$Tc and $^{93}$Ru, see Fig. 3). The values plotted represent an average of all three runs (one at GSI and two at LNL). All $\overline{\mathrm{TR}}(i)$ except $\overline{\mathrm{TR}}(751)$ are consistent with unity, as expected. The error bars include the error on the individual TR for each line and the (small) error on $\overline{\mathrm{DR}}(i \neq 751)$. The 1516 keV line from $^{93}$Tc is not included as it forms a barely-resolved triplet of lines with other radioactive transitions.

Table 1
Double and triple ratios of isomer lines for all three runs. The last column presents the final average over the three runs of the triple ratios.

| $\gamma$ energy (keV) | GSI | | LNL(1) | | LNL(2) | | $\overline{\mathrm{TR}}$(i) |
|---|---|---|---|---|---|---|---|
| | DR($i$) | TR($i$) | DR($i$) | TR($i$) | DR($i$) | TR($i$) | |
| 544($^{93}$Ru) | 0.9990(13) | 1.0004(13) | 0.9965(12) | 1.0017(12) | 0.9989(13) | 1.0010(13) | 1.00107(73) |
| 629($^{93}$Tc) | 1.0002(8) | 1.00160(85) | 0.9993(9) | 0.9996(9) | 0.9990(10) | 1.0002(10) | 1.00055(53) |
| 711($^{93}$Tc) | 0.9990(5) | 1.0004(6) | 0.9944(6) | 0.99970(65) | 0.9982(7) | 0.99930(75) | 0.99989(38) |
| 751($^{93}$Tc) | 0.9963(9) | 0.9977(9) | 0.9936(9) | 0.9989(9) | 0.9972(10) | 0.9984(10) | 0.99833(54) |
| 1392($^{93}$Ru) | 0.9956(14) | 0.9970(14) | 0.9956(14) | 1.00083(14) | 0.9992(16) | 1.0004(16) | 0.99933(84) |
| 1432($^{93}$Tc) | 0.9975(6) | 0.99893(65) | 0.9949(6) | 1.00018(65) | 0.9992(7) | 1.00030(75) | 0.99977(39) |

where the errors shown tare he statistical error and the error associated with the nuclear physics parameters and polarization $p_I$ value (Eq. (1)), respectively.

Preparations are currently in progress for an experiment which will have about a ten times higher count rate. This will be achieved by the use of the newly constructed cluster $\gamma$ detectors and improvements in the transport of both the primary $^{32}$S beam and the $^{93}$Tc beam.

It is interesting to compare our present result with previous measurements involving other nuclear levels (Table 2). The most experimentally convincing (highest accuracy) case of a PNC effect in the decay of a bound nuclear level is the case of the $8^-$ K isomer in $^{180}$Hf [7]. The complex structure of this K isomer precludes a quantitative theoretical analysis leading to conclusions about NN PNC, since it is virtually impossible to compute the overlap of $H_{\mathrm{pnc}}$ with the $|I = 8^-, K = 8\rangle$ and $|I = 8^+, K = 0\rangle$ wave functions. It is presumably also this complex structure of the isomer which gives rise to the extremely large hindrance factor for the transition which made the measurement

Table 2
Summary of PNC measurements in bound nuclear systems. Data for this table are taken from Adelberger and Haxton [3] and references therein. The $^{93}$Tc figure is the result of the present experiment. A recent measurements by Zeps et al. [13] on the *unbound* parity doublet of $0^+$–$0^+$ levels in $^{14}$N yields: $\langle H_{pnc}\rangle$=0.38(28) eV.

| Nucleus | $I^{+-}$ | $\tau(-)$ | $\Delta E$ | Measurement | $P_I$ | Enhancement | $\langle H_{pnc}\rangle$ |
|---|---|---|---|---|---|---|---|
| $^{18}$F | $0^+/0^-$ | 28 ps | 39 keV | $P_\gamma = 8(39)\cdot 10^{-5}$ | | 112 | $\leq$90 meV |
| $^{19}$F | $1/2^+/1/2^-$ | 853 ps | 110 keV | $A_\gamma = -7.4(1.9)\cdot 10^{-5}$ | ~0.7 | 11 | 380 (100) meV |
| $^{21}$Ne | $1/2^+/1/2^-$ | 110 ps | 5.7 keV | $P_\gamma = 80(140)\cdot 10^{-5}$ | | 296 | $\leq$30 meV |
| $^{180}$Hf | $8^+/8^-$ | 7.5 h | 57 keV | $A_\gamma = 1.66(0.18)\cdot 10^{-2}$ | 0.72 | $2\cdot 10^9$ | 1.0(0.1) $\mu$eV |
| $^{93}$Tc | $\frac{17}{2}^+/\frac{17}{2}^-$ | 15 $\mu$s | 0.3 keV | $A_\gamma = 7.7(2.6)\cdot 10^{-4}$ | ~0.15 | 2000 | 0.59(0.19) meV |

possible.

In contrast to $^{180}$Hf, the $^{93}$Tc isomer has a more transparent structure of 5 valence protons outside the $^{88}$Sr core. We have carried out calculations based upon the "best-value" PNC interaction of Desplanques, Donoghue and and Holstein (DDH) [4]. The results in Table 3 are broken down into four isoscalar (IS), five isovector (IV) and two isotensor (IT) components each of which is labeled by the particular meson-nuclear coupling constant to which it is proportional. The method of calculation including the description of the short-range correlations is the same as used in Refs. [6] and [14]. Harmonic-oscillator radial wave functions with $\hbar\omega$ = 8.7 MeV are used. PNC matrix elements between single-particle states which have the same $j$ value but different $\ell$ values pick up a coherent (one-body) contribution from all occupied orbitals and tend to be the terms which dominate PNC observables in light and heavy nuclei. The case of $^{93}$Tc is unique in this regard because this one-body contribution is not allowed by the dominant $1p_{1/2}$ and $0g_{9/2}$ valence wave functions.

Model A is the simple $1p_{1/2}$–$0g_{9/2}$ model space used by Morrison and McKellar [15]. We used the "seniority-conserving" interaction of Glockner and Serduke [9]. The Morrison-McKellar calculations use the PNC interaction of Desplanques and Missimer (DM) which is somewhat older than DDH. But the DM and DDH PNC interactions are similar and the results given in Table 3 (with a total 5.5 meV) are close to those obtained by Morrison and McKellar – both are nearly an order of magnitude larger than the value obtained in the present experiment. We note that the IV terms are small in Model A since the dominant pion-exchange contribution ($IV_1$) has an isospin structure which vanishes for $T$ = 1 two-body

Table 3
PNC matrix elements (in units of meV).

| Term | | Model | | | |
|---|---|---|---|---|---|
| | | A | B | C | D |
| $IS_1$ | $-g_\rho h_\rho^{(0)}(1+\chi_V)$ | 3.05 | 2.39 | 0.17 | |
| $IS_2$ | $-g_\rho h_\rho^{(0)}$ | 0.40 | 0.35 | 0.42 | |
| $IS_3$ | $-g_\omega h_\omega^{(0)}(1+\chi_S)$ | 0.28 | 0.22 | 0.20 | |
| $IS_4$ | $-g_\omega h_\omega^{(0)}$ | 0.20 | 0.18 | 0.01 | |
| $\sum_i IS_i$ | | 3.93 | 3.14 | 0.80 | 0.01 |
| $IV_1$ | $f_\pi g_{\pi NN}$ | 0 | 0 | −4.36 | |
| $IV_2$ | $-g_\rho h_\rho^{(1)} - g_\omega h_\omega^{(1)}$ | 0.13 | 0.11 | 0.07 | |
| $IV_3$ | $-g_\rho h_\rho^{(1)}(1+\chi_V)$ $-g_\omega h_\omega^{(1)}(1+\chi_S)$ | 0.22 | 0.17 | 0.15 | |
| $IV_4$ | $g_\rho h_\rho^{(1)} - g_\omega h_\omega^{(1)}$ | 0 | 0 | −0.06 | |
| $IV_5$ | $-g_\rho h_\rho^{\prime 1}$ | 0 | 0 | −0.07 | |
| $\sum_i IV_i$ | | 0.35 | 0.28 | −4.26 | −4.33 |
| $IT_1$ | $-g_\rho h_\rho^{(2)}$ | 0.13 | 0.12 | 0.14 | |
| $IT_2$ | $-g_\rho h_\rho^{(2)}(1+\chi_V)$ | 1.05 | 0.82 | 1.10 | |
| $\sum_i IT_i$ | | 1.18 | 0.94 | 1.26 | 1.02 |
| $\sum$ | | 5.46 | 4.36 | −2.20 | −3.30 |

configurations. The PNC observables in light nuclei are consistent with an IS contribution which is 0.5 to 1.2 times the DDH best-value [6]. If we were to take the lower value of 0.5, the total PNC matrix element of 3.5 meV is still much larger than experiment. The isotensor contribution (IT) is usually small compared to the IS and IV terms since it does not contribute the the one-body PNC matrix element. In addition, the IT contribution does not contribute to $^{18}$F and $^{19}$F because of isospin selection rules and in the case if $^{14}$N it turns out to be small [16]. The case of $^{93}$Tc is thus the first which we are aware of where the experimental PNC matrix element is comparable to the size of the expected IT contribution.

We now consider Model B where the model space is enlarged to include $0f_{5/2}$, $1p_{3/2}$, $1p_{1/2}$ and $0g_{9/2}$. We have calculated the PNC matrix elements in the full Model B space with the strong interaction of Ji and Wildenthal [10]. The results for the $^{93}$Tc PNC matrix element given in Table 3 are not very different from the Model A results and are still much larger than experiment.

We next examine the effects beyond the space of Model B. The most important excitations to consider are: (a) $1s_{1/2} \rightarrow 1p_{1/2}$, (b) $1p_{1/2} \rightarrow 2s_{1/2}$ and (c) $0g_{9/2} \rightarrow 0h_{9/2}$. These are important because even though the amplitude may be small, in each case the PNC matrix element picks up a coherent contribution from all of the core nucleons. We have made an explicit calculation of contribution (b) by enlarging Model A to include the $2s_{1/2}$ orbital and then allowing one nucleon to be excited into this orbital (Model C). Following again the formalism of Refs. [14] and [6], all of the terms discussed above including the summation over the core nucleons are explicitly taken into account. The model space and interaction are described in [17]. In Table 3 we give the results obtained from this calculation. We indeed find a large change in the two PNC matrix elements, $IS_1$ and $IV_1$, which contribute to the coherent core summation. The additional contribution to $IS_1$ cancels with the zeroth order two-body term. The change in $IV_1$ brings in a new IV contribution. The other PNC operators, in particular the isotensor operator, do not contribute to the core summation and thus are not much effected by the $2s_{1/2}$ admixtures. We are not able to calculate the effects of contributions (a) and (c), however, they should be less important. Contribution (a) should be smaller than (b) because the $1p_{1/2}$ is most filled and the $1s_{1/2} \rightarrow 1p_{1/2}$ excitations are thus blocked. Contribution (c) should be smaller than (b) because the $0g_{9/2}$ proton orbital is not completely filled and because the $0g_{9/2}$–$0h_{9/2}$ energy denominator is larger due to the spin-orbit splitting.

Model B and Model C are two independent enlargements of the simplest Model A. Since the enlargements are both relatively small in amplitude, in the spirit of perturbation theory, we should add the changes obtained from both together. Thus we arrive at the final results labeled Model D in Table 3 which are obtained by $M_D = M_A + [M_B - M_A] + [M_C - M_A]$, where M are the PNC matrix elements. The total Model D value of (IS+IV+IT)=$(0.0 - 4.3 + 1.0) = -3.3$ meV changes sign from Model A but is still larger in magnitude than experiment. However, as mentioned in the introduction, in light nuclei it has been found that the IV term is experimentally strongly suppressed from the DDH value. If we were to reduce the IV contribution by the empirical factor of $0.15 \pm 0.15$ found for light nuclei [6], then the total value would be [IS+IV+IT]=$[0.0 - (0.6 \pm 0.6) + 1.0] = -0.2$ to 1.0 meV in agreement with experiment. It appears that the PNC matrix element may be dominated by the isotensor term, but the theoretical uncertainties in the IS and IV terms must be considered more carefully. In particular, second-order effects, such as the excitation of two neutrons across the $N = 50$ closed shell, should be examined.

One might check the calculation by looking at the E1 strength between the $17/2^-$ and $17/2^+$ levels. This is not known in $^{93}$Tc but is known for the similar pair of levels in $^{95}$Rh [9] where one finds the extremely hindered value of $B(E1) = 6.9 \cdot 10^{-9}$. All E1 matrix elements are zero in Models A and B. Beyond Model B, the E1 strength depends on many more excitations than are important for the PNC matrix element (e.g. $1p_{3/2} \rightarrow 1d_{3/2}$, $1p_{1/2} \rightarrow 1d_{3/2}$, etc.). Unfortunately, a calculation which includes all of the excitations which are important for the E1 matrix elements (including the complete set of excitations which are necessary to remove the spurious states) is much beyond the scope of the present calculations.

In summary, we find that the PNC calculation for $^{93}$Tc leads to potentially interesting conclusions when compared with the small experimental value. The PNC matrix element obtained in the simplest $1p_{1/2}$–$0g_{9/2}$ model space is in itself very stable and much larger than the experimental value. Small admixtures of other orbitals strongly change the result for the IS and IV contributions. The isotensor contribution can be reliably calculated and, compared to other PNC observables, gives a large contribution compared with the experimental value. Agreement with experiment is improved if the IV DDH strength is reduced as observed for light nuclei.

We acknowledge the skillful preparation of the foils by Mr. L. Sapir of the Weizmann Institute and the assistance of the the staff at GSI and LNL during the runs. BAB was supported in part by NSF grant 94-03666.

## References

[1] B.A. Brown, D.B. Fossan, P.M.S. Lesser and A.R. Poletti, Phys. Rev. C 13 (1976) 1194;
B.A. Brown, R.A. Warner, L.E. Young and F.M. Bernthal, Phys. Rev. C 17 (1978) 2040.
[2] B.A. Brown, O. Häusser, T. Faesterman, D. Ward, H.R. Andrews and D. Horn, Nucl. Phys. A 306 (1978) 242.
[3] E.G. Adelberger and W.C. Haxton, Annu. Rev. Nucl. Part. Sci. 35 (1985) 501.
[4] B. Desplanques, J.F. Donoghue and B.R. Holstein, Ann. Phys. (N.Y.) 124 (1980) 449.
[5] G.B. Feldman, G.A. Crawford, J. Dubach and B.R. Holstein, Phys. Rev. C 43 (1991) 863.
[6] M. Horoi and B.A. Brown, Phys. Rev. Lett. 74 (1995) 231.
[7] K.S. Krane, C.E. Olsen, J.R. Sites and W.A. Steyert, Phys. Rev. C 4 (1971) 1906.
[8] J.D. Bowman, G.T. Garvey, M.B. Johnson and G.E. Mitchell, Annu. Rev. Nucl. Part. Sci. 43 (1993) 829.
[9] D.H. Glockner and F.J.P. Serduke, Nucl. Phys. A 220 (1974) 447.
[10] X. Ji and B.H. Wildenthal, Phys. Rev. C 37 (1988) 1256; C 38 (1988) 2849.
[11] C. Broude, G. Goldring, M. Hass, N. Takahashi, S. Hofmann, F.P. Hessberger and V. Ninov, Z. Physik A 336 (1990) 133.
[12] M. Hass, M. Satteson, C.Y. Wu, C. Broude and N. Benczer-Koller, Phys. Rev. C 43 (1991) 2140.
[13] V.J. Zeps, E.G. Adelberger, A. Garcia, C.A. Gosset, H.E. Swanson, W. Haeberli, P.A. Quin and J. Sromicki, Phys. Rev. C 51 (1995) 1494.
[14] B.A. Brown, W.A. Richter and N.S. Godwin, Phys. Rev. Lett. 45 (1980) 1681.
[15] I. Morrison and B.H. McKellar, J. Phys. G 6 (1980) L109.
[16] E.G. Adelberger, P. Hoodbhoy and B.A. Brown, Phys. Rev. C 30 (1984) 456;
M. Horoi, G. Clausnitzer, B.A. Brown and E.K. Warburton, Phys. Rev. C 50 (1994) 775.
[17] B.A. Brown and K. Rykaczewski, Phys. Rev. C 50 (1994) R2270.
[18] H.A. Roth et al., Phys. Rev. C 50 (1994) 1330.